MOX–Report No. 22/2010

Numerical approximation with Nitsche's coupling of transient Stokes'/Darcy's flow problems applied to hemodynamics

Carlo D'Angelo, Paolo Zunino

MOX, Dipartimento di Matematica "F. Brioschi"
Politecnico di Milano, Via Bonardi 9 - 20133 Milano (Italy)

mox@mate.polimi.it http://mox.polimi.it

Numerical approximation with Nitsche's coupling of transient Stokes'/Darcy's flow problems applied to hemodynamics*

Carlo D'Angelo and Paolo Zunino

Abstract

In this work, we consider a time dependent coupled Stokes-Darcy flow problem and study an approximation method based on a unified finite element scheme complemented with implicit time stepping. Our finite element formulation relies on a weighing strategy in which the physical and discretization parameters are taken into account to robustly enforce interface and boundary conditions by means of the Nitsche's method. We prove unconditional absolute stability and optimal convergence of the scheme, and discuss the algebraic properties of the associated discrete problem. Finally, we present numerical experiments confirming the predicted convergence behavior and algebraic properties, and report an application to the computational analysis of blood flow and plasma filtration in arteries after the implantation of a vascular graft.

1 Introduction

The purpose of this work is to set up and analyze a numerical approximation scheme for transient heterogeneous incompressible flows, such as the coupled Stokes'/Darcy's equations. This problem is a simple but yet representative case of the coupled flow problems that arise, for example, in the study of mass transport in the cardiovascular system, where the analysis of blood flow and intramural plasma filtration is important to determine the amount of nutrients, drug or wastes that can be supported or removed to/from tissues neighboring blood vessels. We remand the interested reader to [13] for a general overview. The peculiar nature of the problem demands to apply a spatial discretization technique with corresponding discrete transmission conditions at the interface that are robust with respect to the problem heterogeneity. To pursue this objective we exploit the flexibility of the finite element method. Our main goal is to analyze the interplay between specific finite element schemes that ensure robust approximation of heterogeneous problems and a time advancing technique based on finite differences.

Concerning the founding ideas and the relevant contributions at the basis of the present work, it is not our scope to report a satisfactory review here. We simply restrict to a discussion of the few works that have most closely inspired our approach.

A seminal work for the application and analysis of Nitsche's method to coupled problems is [2], which has been extended to the case of heterogeneous advection

*This work has been supported by the Italian Institute of Technology with the project *NanoBiotechnology - Models and Methods for Local Drug Delivery from Degradable Materials*, and by the ERC Advanced Grant N.227058 *MATHCARD - Mathematical Modelling and Simulation of the Cardiovascular System*.

diffusion equations in [5]. Concerning the migration of these techniques to incompressible flow problems we remand the reader to [4] for a preliminary application and to [10] for for a detailed analysis of a scheme that is closely related to the present one.

For the analysis of stability and convergence of time advancing schemes we apply the classical setting inherited from parabolic problems, for which we refer to [14]. As regards the applications of Nitsche's mortar method for transient coupled problems much fewer literature is available, to our knowledge. For the analysis of coupled parabolic problems we mention [8], although the interface conditions addressed there are significantly different than the ones addressed in our case at the discrete level. Another significant contribution to our research comes from the analysis of stabilized finite element methods for the transient Stokes' problem. This is a vivid research area where, among many others, a relevant contribution to our work is [6].

As previously mentioned, the main purpose of this work is to extend to the transient case a robust finite element scheme for heterogeneous incompressible flow problems. As previously illustrated in [10, 9], the uniform stability and error estimates of the scheme with respect to the magnitude of the problem coefficients depend on the specific choice of the discrete transmission conditions together with a suitable scaling of the natural norm that is applied for the stability and convergence analysis. We will show that for the extension to the time dependent case, this particular weighing and scaling technique represents an advantage with respect to the analysis of the absolute stability, but it introduces some technical difficulties in the derivation of *a-priori* error estimates. More precisely, we observe that for the approximation of transient problems, the natural norm to achieve robustness depends on both characteristic discretization parameters in space and time. This time step dependent norm allows to prove the unconditional stability of the standard backward Euler time advancing scheme with control on both velocity and pressure, for any admissible choice of the initial state. This is indeed a new technique to circumvent the *parabolic-CFL* condition that has been discussed in details in [6]. Another advantage of the analysis in the aforementioned norm consists in the fact that it straightforwardly points out a strategy to set up an optimal preconditioner of the algebraic problem arising at each time step. Evidence of this property, extensively addressed in [9], will be provided by means of numerical experiments.

The manuscript is organized as follows. After addressing the problem set up in section 2, we apply in section 3 a finite difference method for the time discretization and a finite element method to discretize in space. For the sake of simplicity, we restrict to low order schemes, such as backward Euler for the time stepping, while for the construction of a robust finite element method we straightforwardly apply the techniques formerly developed in [10, 9]. Then, in sections 4 and 5 we perform the stability and convergence analysis of the method. We also present numerical experiments to verify the sharpness of the theoretical estimates. Finally, we address the aforementioned application of blood flow and intramural plasma filtration and we evaluate the efficacy of our scheme, from both the points of view of accuracy and computational cost, when applied to a realistic problem that have been studied in the steady regime in [19].

2 The coupling of Stokes/Oseen with Darcy equations

We denote by $\hat{\Omega}_1$ the physical domain occupied by a porous medium, where the flow is governed by Darcy's model, and by $\hat{\Omega}_2$ the domain occupied by a free fluid, modeled for simplicity by Stokes' equation. We assume that $\hat{\Omega}_1$ and $\hat{\Omega}_2$ share an interface denoted with $\hat{\Gamma}$. Let $\partial\hat{\Omega}_i = \hat{\Gamma} \cup \hat{\Gamma}_i^D \cup \hat{\Gamma}_i^N$ be the splitting of each domain boundary into the interface $\hat{\Gamma}$ complemented by Dirichlet and Neumann external boundaries.

Let us denote by $\hat{\mathbf{u}}_i$ the velocity and by $\hat{p}_i$ the pressure (normalized with respect to the fluid density) into each subregion with $i = 1, 2$. Then, we consider the following governing equations,

$$\begin{cases} \hat{\eta}_1 \hat{\mathbf{u}}_1 + \nabla \hat{p}_1 = 0; \quad \nabla \cdot \hat{\mathbf{u}}_1 = 0, \text{ in } \hat{\Omega}_1 \times (0, \hat{T}] \\ \partial_t \hat{\mathbf{u}}_2 - \hat{\nu}_2 \Delta \hat{\mathbf{u}}_2 + \nabla \hat{p}_2 = 0; \quad \nabla \cdot \hat{\mathbf{u}}_2 = 0, \text{ in } \hat{\Omega}_2 \times (0, \hat{T}] \end{cases} \tag{1}$$

to be complemented by suitable initial, boundary and interface conditions. Here, the parameter $\hat{\nu}_2$ denotes the kinematic viscosity of the free fluid and $\hat{\eta}_1$ is the hydraulic resistance of the porous medium. The latter notation relies on the assumption that the porous medium has isotropic and uniform permeability.

We consider the non-dimensional counterpart of problem (1). After introducing the following non-dimensional variables,

$$x = \frac{\hat{x}}{\bar{L}}, \ t = \frac{\hat{t}}{\bar{T}}, \ \mathbf{u} = \frac{\hat{\mathbf{u}}}{\bar{U}}, \ p = \frac{\bar{T}}{\bar{U}\bar{L}} \hat{p}$$

being $\bar{L}, \bar{T}, \bar{U}$ respectively the characteristic length, time and velocity, we choose $\bar{T} = \eta_1^{-1}$ and we set,

$$\alpha^2 = \frac{\hat{\nu}_2}{\bar{L}^2 \hat{\eta}_1}.$$

We note that in all practical applications, the hydraulic impedance of the porous medium, $\hat{\eta}_1$, is a large number. For the problem of intramural plasma filtration in large vessels it can be quantified as $\hat{\eta}_1 = 10^{12} s^{-1}$. As a result of that, the reference time $\bar{T}$ turns out to be extremely small, and consequently the non-dimensional final time $T = \hat{T}/\bar{T}$ becomes very large. Under these conditions, an unconditionally stable numerical scheme that is effective in the large time step regime seems to be the most effective choice. The development of such scheme is exactly the purpose of this work.

From now on, all symbols without the superscript $\hat{}$ will denote non-dimensional quantities. The non-dimensional formulation is at the basis of our analysis and consists in a steady Darcy's problem,

$$\mathbf{u}_1 + \nabla p_1 = \mathbf{0}, \text{ in } \Omega_1 \times (0, T], \tag{2a}$$
$$\nabla \cdot \mathbf{u}_1 = 0, \text{ in } \Omega_1 \times (0, T], \tag{2b}$$
$$\mathbf{u}_1 \cdot \mathbf{n}_1 = 0 \text{ on } \Gamma_1^D \times (0, T], \tag{2c}$$
$$\mathbf{n}_1 \cdot \sigma_1 \mathbf{n}_1 = 0 \text{ on } \Gamma_1^N \times (0, T], \tag{2d}$$

coupled with a transient Stokes' problem,

$$\partial_t \mathbf{u}_2 - \alpha^2 \Delta \mathbf{u}_2 + \nabla p_2 = \mathbf{0}, \text{ in } \Omega_2 \times (0, T], \tag{3a}$$
$$\nabla \cdot \mathbf{u}_2 = 0, \text{ in } \Omega_2 \times (0, T], \tag{3b}$$
$$\mathbf{u}_2 = \mathbf{0} \text{ on } \Gamma_2^D \times (0, T], \tag{3c}$$
$$\sigma_2 \mathbf{n}_2 = \mathbf{0} \text{ on } \Gamma_2^N \times (0, T], \tag{3d}$$
$$\mathbf{u}_2(0, x) = \mathbf{u}_{2,0}(x), \text{ in } \Omega_2 \tag{3e}$$

by means of the following interface conditions,

$$\mathbf{n}_2^T \sigma_2 \mathbf{n}_2 - \mathbf{n}_1^T \sigma_1 \mathbf{n}_1 = 0 \text{ on } \Gamma \times (0, T], \tag{4a}$$
$$\mathbf{u}_2 \cdot \mathbf{n}_2 + \mathbf{u}_1 \cdot \mathbf{n}_1 = 0 \text{ on } \Gamma \times (0, T], \tag{4b}$$
$$\mathbf{n}_2 \times \mathbf{u}_2 = \mathbf{0} \text{ on } \Gamma \times (0, T], \tag{4c}$$

where $\sigma_2 = p_2 I - \alpha^2 \nabla \mathbf{u}_2$, $\sigma_1 = p_1 I$ are the Cauchy stress tensors (we denote by I the identity tensor) and we introduce the additional notation $\alpha_1 = 0$, $\alpha_2 = \alpha^2$. As usual, let us denote with $\mathbf{n}_i$ the outward unit vector on $\partial\Omega_i$ and with $\mathbf{n}$ a normal unit vector on Γ. The orientation of $\mathbf{n}$ is arbitrary and does not affect our method.

In order to address the variational formulation of (2), (3), (4) we define,

$$\mathbf{V}_1 := \{\mathbf{v} \in H_{\mathrm{div}}(\Omega_1) : \ \mathbf{v} \cdot \mathbf{n}_1|_{\Gamma_1^D} = 0\}, \quad Q_1 := H^1(\Omega_1),$$
$$\mathbf{V}_2 := \{\mathbf{v} \in [H^1(\Omega_2)]^d : \ \mathbf{v}|_{\Gamma_2^D} = \mathbf{0}\}, \quad Q_2 := L^2(\Omega_2),$$

and $\mathbf{V} := \mathbf{V}_i \oplus \mathbf{V}_2$, $Q := Q_1 \oplus Q_2$, being $H_{\mathrm{div}}(\Omega_1) := \{\mathbf{v} \in [L^2(\Omega_1)]^d : \ \nabla \cdot \mathbf{v} \in L^2(\Omega_1)\}$, and we introduce the following bilinear forms and linear functionals,

$$\mathcal{A}(\mathbf{u}, \mathbf{v}) := \int_{\Omega_1} \mathbf{u}_1 \cdot \mathbf{v}_1 + \int_{\Omega_2} \alpha_2 \nabla \mathbf{u}_2 : \nabla \mathbf{v}_2$$

$$\mathcal{B}(q, \mathbf{u}) := \int_{\Omega_1} q_1 \nabla \cdot \mathbf{u}_1 + \int_{\Omega_2} q_2 \nabla \cdot \mathbf{u}_2 + \int_{\Gamma} q_1 \big(\mathbf{u}_1 \cdot \mathbf{n} - \mathbf{u}_2 \cdot \mathbf{n}\big)$$
$$\mathcal{F}(\mathbf{v}; t) := \int_{\Omega_2} \mathbf{f}_2 \cdot \mathbf{v}_2 + \int_{\Omega_1} \mathbf{f}_1 \cdot \mathbf{v}_1 \text{ with } \mathbf{f}_i \in L^2\big((0,T]; \mathbf{L}^2(\Omega_i)\big)$$

Let us denote with $\mathcal{H}_{\mathrm{div},2}$ the space of velocity fields that are weakly solenoidal, i.e. $\mathcal{H}_{\mathrm{div},2} := \{\mathbf{v} \in \mathbf{V} : \int_{\Omega_2} q_2 \nabla \cdot \mathbf{v}_2 = 0, \ \forall q_2 \in Q_2\}$. Given $\mathbf{u}_{2,0} \in \mathcal{H}_{\mathrm{div},2}$, the weak formulation of the coupled problem (2), (3), (4) consists in finding $\mathbf{u} \in L^2\big((0,T]; \mathbf{V}\big)$, $p \in L^2\big((0,T]; Q\big)$ such that

$$\begin{cases} \big(\partial_t \mathbf{u}_2, \mathbf{v}_2\big)_{\Omega_2} + \mathcal{A}(\mathbf{u}, \mathbf{v}) + \mathcal{B}(p, \mathbf{v}) = \mathcal{F}(\mathbf{v}; t), \ \forall \mathbf{v} \in \mathbf{V} \\ \mathcal{B}(q, \mathbf{u}) = 0, \forall q \in Q \\ \mathbf{u}_2(t=0) = \mathbf{u}_{2,0} \end{cases} \tag{5}$$

where $(\cdot, \cdot)_{\Omega_i}$ denotes the L^2 inner product on Ω_i. Setting $\mathcal{C}\big((\mathbf{u}, p), (\mathbf{v}, q)\big) := \mathcal{A}(\mathbf{u}, \mathbf{v}) + \mathcal{B}(p, \mathbf{v}) - \mathcal{B}(q, \mathbf{u})$ and introducing for the sake of generality $\mathcal{G}(\mathbf{v}, q; t) := \mathcal{F}(\mathbf{v}; t)$ and $\mathbf{W} := \mathbf{V} \times Q$, problem (5) can be also rewritten as,

$$\big(\partial_t \mathbf{u}_2, \mathbf{v}_2\big)_{\Omega_2} + \mathcal{C}\big((\mathbf{u}, p), (\mathbf{v}, q)\big) = \mathcal{G}(\mathbf{v}, q; t), \ \forall (\mathbf{v}, q) \in \mathbf{W}.$$

Note that the pressure will be uniquely determined by the prescribed external stresses, provided that $\Gamma_i^N \neq \emptyset$. The additional regularity of the pressure on Ω_1, namely $p_1 \in H^1(\Omega_1)$, is required to make sure that the interface terms $\int_\Gamma p_1 \big(\mathbf{v}_2 \cdot \mathbf{n} - \mathbf{v}_1 \cdot \mathbf{n}\big)$ and $\int_\Gamma q_1 \big(\mathbf{u}_2 \cdot \mathbf{n} - \mathbf{u}_1 \cdot \mathbf{n}\big)$ are well defined. Furthermore, the forthcoming analysis relies on several additional regularity assumptions. For the sake of clarity, they are collected below and we will recall them when needed. In order to ensure that the discrete bilinear forms make sense for the exact weak solution of the problem, we require that,

$$(\mathbf{u}_2, p_2) \in C^0\big((0,T]; \mathbf{H}^{\frac{3}{2}+\epsilon}(\Omega_2) \times H^{\frac{1}{2}+\epsilon}(\Omega_2)\big), \text{ for any } \epsilon > 0, \tag{6}$$

while for the error analysis of the space discretization we need $(\mathbf{u}_i, p_i) \in L^\infty\big((0,T]; (\mathbf{H}^2(\Omega_i) \cap \mathbf{V}_i) \times H^1(\Omega_i)\big)$ and $\partial_t \mathbf{u}_2 \in L^2\big((0,T]; \mathbf{H}^2(\Omega_2)\big)$, $\partial_t p_2 \in L^2\big((0,T]; H^1(\Omega_2)\big)$. For a discussion of the requirements on the domain and on the data that make sure that these assumptions hold true we refer to [11]. Finally, we assume that $\mathbf{u}_{2,0} \in \mathbf{H}^2(\Omega_2)$.

3 Numerical approximation

To set up our numerical discretization method we restrict to simple low order schemes, both for the time and space discretization. Concerning time discretization, we exploit the backward Euler scheme. We estimate that the extension of our analysis to second order BDF schemes could be developed following the lines of [6]. Concerning the space discretization, our scheme is inspired to [4], with the subsequent improvements and generalizations proposed in [10, 9].

3.1 Finite difference time discretization

Given a sequence of evenly spaced times t_n, characterized by a constant time step τ, for the time discretization we consider a backward Euler scheme that is characterized by the following approximation of the time derivative at time t^n

$$D_\tau \mathbf{u}^n := \frac{\mathbf{u}^n - \mathbf{u}^{n-1}}{\tau},$$

and leads to the following sequence of problems: given $(\mathbf{u}_i^{n-1}, p_i^{n-1})$ for $i = 1, 2$ find $(\mathbf{u}_i^n, p_i^n)$ such that

$$\mathbf{u}_1^n + \nabla p_1^n = \mathbf{0}; \quad \nabla \cdot \mathbf{u}_1^n = 0, \text{ in } \Omega_1 \tag{7a}$$

$$D_\tau \mathbf{u}_2^n - \alpha^2 \Delta \mathbf{u}_2^n + \nabla p_2^n = \mathbf{0}; \quad \nabla \cdot \mathbf{u}_2^n = 0, \text{ in } \Omega_2 \tag{7b}$$

complemented with the initial, interface and boundary conditions already introduced in (2), (3) and (4).

3.2 Finite element space discretization

We assume that each $\Omega_i \subset \mathbb{R}^d$ is a convex polygonal domain, equipped with a family of quasi-uniform triangulations $\mathcal{T}_{h,i}$ made of affine simplexes K that are conforming on Γ. Let h be their characteristic size. We also denote with $\mathcal{F}_{h,i}$ the set of all interior faces F of $\mathcal{T}_{h,i}$, and set $\mathcal{T}_h = \cup_i \mathcal{T}_{h,i}$, $\mathcal{F}_h = \cup_i \mathcal{F}_{h,i}$.

For the local approximation on each subregion we consider a ($\mathbb{P}^1$, $\mathbb{P}^0$) finite element pair for velocity and pressure respectively,

$$V_{h,i} := \{v_h \in V(\Omega_i) \cap C^0(\Omega_i) \ : \ v_h|_K \in \mathbb{P}^1(K), \ \forall K \in \mathcal{T}_{h,i}\}, \quad \mathbf{V}_{h,i} = [V_{h,i}]^d,$$
$$Q_{h,i} := \{q_h \in L^2(\Omega_i) \ : \ q_h|_K \in \mathbb{P}^0(K), \ \forall K \in \mathcal{T}_{h,i}\}.$$

As global approximation spaces, we consider $\mathbf{V}_h := \mathbf{V}_{h,1} \oplus \mathbf{V}_{h,2}$, $Q_h := \big(Q_{h,1} \oplus Q_{h,2}\big)$ and $\mathbf{W}_h := \mathbf{V}_h \times Q_h$.

We define the jump of any finite element function ϕ_h across any (internal) face F of the computational grid in the usual way,

$$[\![\phi_h]\!](\mathbf{x}) := \lim_{\delta \to 0} [\phi_h(\mathbf{x} - \delta \mathbf{n}_F) - \phi_h(\mathbf{x} + \delta \mathbf{n}_F)], \quad \mathbf{x} \in F.$$

Here, ϕ_h can be a scalar Q_h function or a vector $\mathbf{V}_h$ function. The orientation of the normal $\mathbf{n}_F$ is arbitrary and does not influence the method. Finally, we denote $h_F = \text{diam}(F)$ the diameter of any face F. With little abuse of notation, we also denote h_F a piecewise constant function defined on $\mathcal{F}_h$, taking the value diam(F) on each face F. We also define the weighted and conjugate weighted averages on Γ,

$$\{\phi_h\}_w := \sum_{i=1,2} w_i \phi_{h,i}, \quad \{\phi_h\}^w := \sum_{i=1,2} \bar{w}_i \phi_{h,i},$$

where $w = (w_2, w_1)$ are suitable weights, such that $w_2 + w_1 = 1$, and $\bar{w}_i = 1 - w_i$ are the conjugate weights. Finally $\{\phi_h\}$ will denote the standard arithmetic average. Setting $\mu_1 = 1,\ \mu_2 = \alpha_2 + \tau^{-1}$ we observe that the weights may depend on α_i, μ_i. In particular, the penalty term that we will introduce to enforce the continuity of the normal velocity at the interface will be scaled by the quantity $\{\mu\}_w$. We observe that μ_2 becomes arbitrarily large for a small time step τ, which is a limitation for the analysis of the convergence properties of the scheme. For this reason, in Lemma 5.1 we will select the weights such that $\{\mu\}_w$ is upper bounded for any value of τ.

To set up our finite element scheme, we start from the following discrete *local* bilinear forms,

$$a_1(\mathbf{u}_{h,1}, \mathbf{v}_{h,1}) := \int_{\Omega_1} \mathbf{u}_{h,1} \cdot \mathbf{v}_{h,1} + \int_{\Gamma_1^D} \gamma_u h_F^{-1} \mu_1 (\mathbf{u}_{h,1} \cdot \mathbf{n}_1)(\mathbf{v}_{h,1} \cdot \mathbf{n}_1),$$

$$\begin{aligned} a_2(\mathbf{u}_{h,2}, \mathbf{v}_{h,2}) := &\int_{\Omega_2} \alpha_2 \nabla \mathbf{u}_{h,2} : \nabla \mathbf{v}_{h,2}, \\ &+ \int_{\Gamma_2^D} \gamma_u h_F^{-1} \Big[\alpha_2 (\mathbf{u}_{h,2} \cdot \mathbf{v}_{h,2}) + \mu_2 (\mathbf{u}_{h,2} \cdot \mathbf{n})(\mathbf{v}_{h,2} \cdot \mathbf{n}) \Big] \\ &- \int_{\Gamma_2^D} \Big[\alpha_2 \nabla \mathbf{u}_{h,2} \mathbf{n}_2 \cdot \mathbf{v}_{h,2} + \alpha_2 \nabla \mathbf{v}_{h,2} \mathbf{n}_2 \cdot \mathbf{u}_{h,2} \Big] \\ &+ \int_{\Gamma} \gamma_u h_F^{-1} \alpha_2 (\mathbf{n}_2 \times \mathbf{u}_{h,2}) \cdot (\mathbf{n}_2 \times \mathbf{v}_{h,2}), \end{aligned}$$

$$b_i(p_{h,i}, \mathbf{v}_{h,i}) := -\int_{\Omega_i} p_{h,i} \nabla \cdot \mathbf{v}_{h,i} + \int_{\Gamma_i^D} p_{h,i} \mathbf{v}_{h,i} \cdot \mathbf{n}_i,$$

$$j_i(p_{h,i}, q_{h,i}) := \int_{\mathcal{F}_{h,i}} \gamma_p h_F \mu_i^{-1} [\![p_{h,i}]\!] [\![q_{h,i}]\!],$$

where γ_u and γ_p are constant parameters that will be chosen large enough to guarantee the stability of the numerical discretization scheme (see Lemma 4.1 and Theorem 4.1). At the discrete level, to couple subproblems (2) and (3) we introduce suitable *matching operators*, which derive from the interface conditions (4),

$$\begin{aligned} c(\mathbf{u}_h, \mathbf{v}_h) := \int_{\Gamma} \Big(&\gamma_u h_F^{-1} \{\mu\}_w [\![\mathbf{u}_h \cdot \mathbf{n}]\!] [\![\mathbf{v}_h \cdot \mathbf{n}]\!] \\ &- \{\alpha \mathbf{n}^T \nabla \mathbf{u}_h \mathbf{n}\}_w [\![\mathbf{v}_h \cdot \mathbf{n}]\!] - \{\alpha \mathbf{n}^T \nabla \mathbf{v}_h \mathbf{n}\}_w [\![\mathbf{u}_h \cdot \mathbf{n}]\!] \Big), \end{aligned}$$

$$d(p_h, \mathbf{v}_h) := \int_{\Gamma} \{p_h\}_w [\![\mathbf{v}_h \cdot \mathbf{n}]\!].$$

Summing up all these terms we obtain the following *global* bilinear forms,

$$\mathcal{A}_h(\mathbf{u}_h, \mathbf{v}_h) := \sum_{i=1,2} a_i(\mathbf{u}_{h,i}, \mathbf{v}_{h,i}) + c(\mathbf{u}_h, \mathbf{v}_h),$$

$$\mathcal{B}_h(p_h, \mathbf{v}_h) := \sum_{i=1,2} b_i(p_{h,i}, \mathbf{v}_{h,i}) + d(p_h, \mathbf{v}_h),$$

$$\mathcal{J}_h(p_h, q_h) := \sum_{i=1,2} j_i(p_{h,i}, q_{h,i}),$$

$$\mathcal{C}_h((\mathbf{u}_h, p_h), (\mathbf{v}_h, q_h)) := \mathcal{A}_h(\mathbf{u}_h, \mathbf{v}_h) + \mathcal{B}_h(p_h, \mathbf{v}_h) - \mathcal{B}_h(q_h, \mathbf{u}_h) + \mathcal{J}_h(p_h, q_h).$$

We notice that the finite element scheme characterized by $\mathcal{C}_h((\mathbf{u}_h, p_h), (\mathbf{v}_h, q_h))$ is a particular instance of the more general case addressed [9].

To properly set up problem (9), an initial condition $\mathbf{u}_{h,2}^0$ is needed. We denote with $\pi_h : \mathbf{H}^1(\Omega_2) \to \mathbf{V}_{h,2}$ the standard L^2 projection from $\mathbf{H}^1(\Omega_2)$ into $\mathbf{V}_{h,2}$. Then, we choose $\mathbf{u}_{h,2}^0 = \pi_h \mathbf{u}_{2,0}$ with the well known stability and approximation properties,

$$\|\pi_h \mathbf{v}\|_{0,\Omega_2} \lesssim \|\mathbf{v}\|_{0,\Omega_2}, \quad \|(I - \pi_h)\mathbf{v}\|_{0,\Omega_2} \lesssim h|\mathbf{v}|_{1,\Omega_2},$$

where $\lesssim$ and $\gtrsim$ denote from now on inequalities with generic constants C that are independent on the mesh characteristic size, the time step and the problem coefficients α_i, μ_i. Many other approximation techniques may be applied for the definition of $\mathbf{u}_{h,2}^0$, one of the advantages of our approach is that it does not require any restriction to this choice except from stability and first order accuracy.

Then, for each time $t \in (0, T]$ the semidiscrete problem requires to find $\mathbf{u}_h(t), p_h(t)$ such that

$$\begin{cases} \big(\partial_t \mathbf{u}_{h,2}(t), \mathbf{v}_{h,2}\big)_{\Omega_2} + \mathcal{C}_h((\mathbf{u}_h(t), p_h(t)), (\mathbf{v}_h, q_h)) \\ \qquad\qquad = \mathcal{G}(\mathbf{v}_h, q_h; t), \ \forall (\mathbf{v}_h, q_h) \in \mathbf{W}_h, \\ \mathbf{u}_{h,2}(t=0) = \mathbf{u}_{h,2}^0. \end{cases} \tag{8}$$

Given $\mathcal{G}^n(\mathbf{v}_h, q_h) := \mathcal{G}(\mathbf{v}_h, q_h; t^n)$ and $\mathbf{u}_{h,2}^0$ for any $n > 0$, the fully discrete problem consists to find $\mathbf{u}_h^n, p_h^n$ such that

$$\big(D_\tau \mathbf{u}_{h,2}^n, \mathbf{v}_{h,2}\big)_{\Omega_2} + \mathcal{C}_h\big((\mathbf{u}_h^n, p_h^n), (\mathbf{v}_h, q_h)\big) = \mathcal{G}^n\big(\mathbf{v}_h, q_h\big). \tag{9}$$

For notational convenience we also introduce

$$\mathcal{C}_h^\tau\big((\mathbf{u}_h, p_h), (\mathbf{v}_h, q_h)\big) := \tau^{-1}\big(\mathbf{u}_{h,2}, \mathbf{v}_{h,2}\big)_{\Omega_2} + \mathcal{C}_h\big((\mathbf{u}_h, p_h), (\mathbf{v}_h, q_h)\big),$$

which is the bilinear form that defines the algebraic problem to be solved at each time step. We notice that the boundedness, positivity and stability properties that might be proved for $\mathcal{C}_h((\mathbf{u}_h, p_h), (\mathbf{v}_h, q_h))$ can be straightforwardly extended to $\mathcal{C}_h^\tau\big((\mathbf{u}_h, p_h), (\mathbf{v}_h, q_h)\big)$.

4 Stability analysis

The aim of this section is to prove that the backward Euler time advancing scheme, i.e. (7), combined with the finite element method characterized by $\mathcal{C}_h((\mathbf{u}_h, p_h), (\mathbf{v}_h, q_h))$ gives rise to an A-stable scheme. This is an expected result; anyway it is necessary to address the error analysis of our method.

The basic tools to pursue this analysis are the boundedness and stability properties of the discrete bilinear forms defining the selected finite element method. For the sake of clarity, we simply report such general properties in Lemma 4.1, referring to [9] and [10] for detailed proofs.

4.1 Basic notation, definitions and general properties

Let us start introducing the following auxiliary norms,

$$\|\mathbf{v}_{h,i}\|^2_{\pm\frac{1}{2},h,\Sigma} := \int_\Sigma h_F^{\mp 1} \mathbf{v}_h^2, \quad \|[\![q_{h,1}]\!]\|_{\pm\frac{1}{2},h,\mathcal{F}_{h,i}} := \int_{\mathcal{F}_{h,i}} h_F^{\mp 1} [\![q_{h,1}]\!]^2,$$

whose motivation is made clear by the following inverse inequalities (see for instance [18]),

$$h_F^{\frac{1}{2}} \|v_h\|_{0,F} \lesssim \|v_h\|_{0,K}, \quad h_K \|\nabla v_h\|_{0,K} \lesssim \|v_h\|_{0,K}.$$

Then, the natural norms that will be employed for the analysis of our method are,

$$|||\mathbf{v}_h|||^2 := \|\mu_1^{\frac{1}{2}}\mathbf{v}_{h,1}\|^2_{0,\Omega_1} + \|\alpha_2^{\frac{1}{2}}\nabla\mathbf{v}_{h,2}\|^2_{0,\Omega_2} + \|\alpha_2^{\frac{1}{2}}\mathbf{v}_{h,2}\|^2_{\frac{1}{2},h,\Gamma_2^D} + \|\alpha_2^{\frac{1}{2}}\mathbf{n}_2\times\mathbf{v}_{h,2}\|^2_{\frac{1}{2},h,\Gamma},$$
$$|||\mathbf{v}_h|||^2_\tau := |||\mathbf{v}_h|||^2 + \|\tau^{-\frac{1}{2}}\mathbf{v}_{h,2}\|^2_{0,\Omega_2},$$

$$|||(\mathbf{v}_h,q_h)|||^2 := |||\mathbf{v}_h|||^2 + \|\{\mu\}_w^{\frac{1}{2}}[\![\mathbf{v}_h]\!]\cdot\mathbf{n}\|^2_{+\frac{1}{2},h,\Gamma}$$
$$+\sum_{i=1,2}\Big[\|\mu_i^{\frac{1}{2}}\nabla\cdot\mathbf{v}_{h,i}\|^2_{0,\Omega_i} + \|\mu_i^{\frac{1}{2}}\mathbf{v}_{h,i}\cdot\mathbf{n}\|^2_{+\frac{1}{2},h,\Gamma_i^D} + \|\mu_i^{-\frac{1}{2}}q_{h,i}\|^2_{0,\Omega_i} + \|\mu_i^{-\frac{1}{2}}[\![q_h]\!]\|^2_{-\frac{1}{2},h,\mathcal{F}_{h,i}}\Big],$$

and we also define $|||(\mathbf{v}_h,q_h)|||^2_\tau$, where the term $|||\mathbf{v}_h|||^2$ is replaced by $|||\mathbf{v}_h|||^2_\tau$. We observe that in the definition of $|||(\mathbf{v}_h,q_h)|||$ the divergence and the pressure terms have been suitably scaled with respect to the coefficients μ_i (more precisely μ_2 since $\mu_1=1$). This technique will help us to obtain robust stability and error estimates that are independent on the coefficients of the problem. In particular, we observe that the terms proportional to μ_2^{-1} vanish when $\tau\to 0$. For this reason, we say that our analysis holds with a *relaxed* L^2 pressure norm.

Lemma 4.1 (General properties)
(Consistency) *Let* $(\mathbf{u}(t),p(t))$ *be the weak solution of the coupled problem* (5) *satisfying the regularity assumption* (6)*. Then, we have:*

$$\big(\partial_t\mathbf{u}_2(t_n),\mathbf{v}_{h,2}\big) + \mathcal{C}_h((\mathbf{u}(t_n),p(t_n)),(\mathbf{v}_h,q_h)) = \mathcal{G}^n(\mathbf{v}_h,q_h),\ \forall(\mathbf{v}_h,q_h)\in\mathbf{W}_h.$$

(Boundedness) *For all* $(\mathbf{u}_h,p_h)$, $(\mathbf{v}_h,q_h)$ *and for any admissible weights* w_i *we have:*

$$\mathcal{C}_h((\mathbf{u}_h,p_h),(\mathbf{v}_h,q_h)) \lesssim |||\mathbf{u}_h,p_h|||\,|||\mathbf{v}_h,q_h|||,$$
$$\mathcal{C}_h^\tau((\mathbf{u}_h,p_h),(\mathbf{v}_h,q_h)) \lesssim |||\mathbf{u}_h,p_h|||_\tau\,|||\mathbf{v}_h,q_h|||_\tau.$$

(Positivity) *Provided that* γ_u *is large enough and for any admissible weights* w_i*, there exists a positive constant* C_{pos}*, independent of* h*,* τ*,* α_i*,* μ_i*, such that, for all* $(\mathbf{v}_h,q_h)$*:*

$$\mathcal{C}_h((\mathbf{v}_h,q_h),(\mathbf{v}_h,q_h)) - \mathcal{J}_h(q_h,q_h)$$
$$\geq C_{pos}\Big[|||\mathbf{v}_h|||^2 + \sum_{i=1,2}\|\mu_i^{\frac{1}{2}}\mathbf{v}_{h,i}\cdot\mathbf{n}\|^2_{+\frac{1}{2},h,\Gamma_i^D} + \|\{\mu\}_w^{\frac{1}{2}}[\![\mathbf{v}_h]\!]\cdot\mathbf{n}\|^2_{+\frac{1}{2},h,\Gamma}\Big],$$

$$\mathcal{C}_h^\tau((\mathbf{v}_h,q_h),(\mathbf{v}_h,q_h)) - \mathcal{J}_h(q_h,q_h)$$
$$\geq C_{pos}\Big[|||\mathbf{v}_h|||^2_\tau + \sum_{i=1,2}\|\mu_i^{\frac{1}{2}}\mathbf{v}_{h,i}\cdot\mathbf{n}\|^2_{+\frac{1}{2},h,\Gamma_i^D} + \|\{\mu\}_w^{\frac{1}{2}}[\![\mathbf{v}_h]\!]\cdot\mathbf{n}\|^2_{+\frac{1}{2},h,\Gamma}\Big].$$

(Global stabilized inf-sup condition) *Provided that* $\Gamma_i^N\neq\emptyset$ *for* $i=1,2$*, for all* $p_h\in Q_h$ *there exists* $\mathbf{v}_{p,h}\in\mathbf{V}_h\cap H^1_{\Gamma^D}(\Omega)$ *such that,*

$$\mathcal{B}_h(p_h,\mathbf{v}_{p,h}) \gtrsim \|\mu^{-\frac{1}{2}}p_h\|^2_{0,\Omega} - C\|\mu^{-\frac{1}{2}}[\![p_h]\!]\|^2_{-\frac{1}{2},h,\mathcal{F}_h},$$
$$\|\mu^{\frac{1}{2}}\mathbf{v}_{p,h}\|_{1,\Omega} \lesssim \|\mu^{-\frac{1}{2}}p_h\|_{0,\Omega},$$

where C *is a positive constant independent of* h*,* τ*,* α_i*,* μ_i*.*

Proof. For the consistency of the method, we notice that the presence of the evolution term $\big(\partial_t\mathbf{u}_2(t_n),\mathbf{v}_{h,2}\big)$ is irrelevant, because it has not been discretized yet. Thus, the consistency of the semidiscrete problem (8) is equivalent to its steady counterpart that has been addressed in [9], Lemma 2.1. This is also the reference to which we remand the reader for an extended proof of the boundedness and stability properties. □

4.2 Stability analysis for the fully-implicit time advancing scheme

In the following result we first apply an energy argument to problem (9) with the aim of proving the unconditional stability of the fully implicit time advancing scheme in the natural mesh dependent norm for the velocity. This result mimics the classical energy estimate for parabolic problems in $L^2\big((0,T];H^1(\Omega)\big)\cap L^\infty\big((0,T];L^2(\Omega)\big)$. We also obtain some control of the discrete time derivative. However, this part of the estimate is suboptimal, because the control over the discrete time derivative is lost for very small time steps. As put into evidence in [6] this affects the control of the pressure, because the application of the inf-sup condition (see Lemma 4.1) allows to control the L^2 norm of the pressure in terms of the discrete time derivative. Combining these observations, we expect that the stability estimate for the pressure variable may not be robust in the small time step regime. This classical setting has been recently modified by [6], where a new estimate for the discrete time derivative has been obtained, provided that the discrete initial velocity is selected as the Ritz projection of the exact velocity field. Under this condition, the robust control of the pressure is recovered in the L^2 norm.

In this work, we propose a technique to work around the problem of the robustness of the pressure estimate. It consists on suitably scaling the pressure norm, such that the stability estimate turns out to be unconditionally robust for both velocity and pressure. We notice that this result does not contradict the aforementioned observations about the instability of the pressure in the small time step regime, because in our case the control of the pressure is relaxed with respect to the standard analysis in the L^2 norm.

Theorem 4.1 (Stability) *The discrete problem* (9) *is A-stable. More precisely, under the assumptions of Lemma 4.1, for all* $n=0,1,\dots,N_\tau=\frac{T}{\tau}$ *we have*

$$\|\mathbf{u}_{h,2}^n\|^2_{0,\Omega_2}+\tau^2\sum_{k=1}^n\|D_\tau\mathbf{u}_{h,2}^k\|^2_{0,\Omega_2}+\tau\sum_{k=1}^n|||\mathbf{u}_h^k|||^2 \lesssim \|\mathbf{u}_{h,2}^0\|^2_{0,\Omega_2}+\tau\sum_{k=1}^n|||\mathcal{G}^k|||^2 \qquad (10)$$

$$\|\mathbf{u}_{h,2}^n\|^2_{0,\Omega_2}+\tau^2\sum_{k=1}^n\|D_\tau\mathbf{u}_{h,2}^k\|^2_{0,\Omega_2}+\tau\sum_{k=1}^n|||\mathbf{u}_h^n,p_h^n|||^2 \lesssim \|\mathbf{u}_{h,2}^0\|^2_{0,\Omega_2}+\tau\sum_{k=1}^n|||\mathcal{G}^k|||^2 \qquad (11)$$

where $|||\mathcal{G}^n|||:=\sup_{(\mathbf{v}_h,q_h)\in\mathbf{W}_h}\{\mathcal{G}^n(\mathbf{v}_h,q_h):\ |||\mathbf{v}_h,q_h|||\le 1\}$.

Proof. We take $(\mathbf{v}_h^n,q_h^n)=(\mathbf{u}_h^n,p_h^n)+(\delta_2\mathbf{v}_{p,h}^n,0)+(0,\delta_3\mu_i\nabla\cdot\mathbf{u}_{h,i}^n)$ in (9), where δ_i are sufficiently small parameters, and we separately analyze the corresponding terms.

First term. Exploiting the positivity property in Lemma 4.1 we obtain,

$$\mathcal{C}_h\big((\mathbf{u}_h^n,p_h^n),(\mathbf{u}_h^n,p_h^n)\big)\ge C_{pos}\Big[|||\mathbf{u}_h^n|||^2+\|\{\mu\}_w^{\frac12}[\![\mathbf{u}_h^n]\!]\cdot\mathbf{n}\|^2_{+\frac12,h,\Gamma} + \|\mu^{\frac12}\mathbf{u}_h^n\cdot\mathbf{n}\|^2_{+\frac12,h,\Gamma^D}+\gamma_p\|\mu^{-\frac12}[\![p_h^n]\!]\|^2_{-\frac12,h,\mathcal{F}_h}\Big]$$

and we observe that

$$\left(D_\tau \mathbf{u}_h^n, \mathbf{u}_h^n\right)_{\Omega_2} = \frac{1}{2} D_\tau \|\mathbf{u}_{h,2}^n\|_{0,\Omega_2}^2 + \frac{\tau}{2} \|D_\tau \mathbf{u}_{h,2}^n\|_{0,\Omega_2}^2 .$$

Then, combining the previous estimates by means of the Young inequality and summing up over the time advancing index we obtain (10).

Second term. Exploiting the global stabilized inf-sup condition and the estimate $\mathcal{A}_h(\mathbf{u}_h^n, \mathbf{v}_{p,h}^n) \le |||\mathbf{u}_h^n|||\, |||\mathbf{v}_{p,h}^n||| \lesssim \epsilon_2 |||\mathbf{u}_h^n|||^2 + \epsilon_2^{-1} \|\mu^{-\frac{1}{2}} p_h^n\|_{0,\Omega}^2$, for any $\epsilon_2 > 0$ we obtain,

$$\mathcal{C}_h((\mathbf{u}_h^n, p_h^n), (\delta_2 \mathbf{v}_{p,h}^n, 0)) \gtrsim \delta_2 \Big[(1-\epsilon_2) \|\mu^{-\frac{1}{2}} p_h^n\|_{0,\Omega}^2 \\ - C \|\mu^{-\frac{1}{2}} [\![p_h^n]\!]\|_{-\frac{1}{2},h,\mathcal{F}_h}^2 - \epsilon_2^{-1} |||\mathbf{u}_h^n|||^2 \Big].$$

Moreover, reminding that $\mu_2 = \alpha_2 + \tau^{-1}$,

$$\left(D_\tau \mathbf{u}_{h,2}^n, \delta_2 \mathbf{v}_{p,h,2}^n\right)_{\Omega_2} \lesssim \delta_2 \epsilon_2^{-1} \mu_2^{-1} \|D_\tau \mathbf{u}_{h,2}^n\|_{0,\Omega_2}^2 + \delta_2 \epsilon_2 \|\mu_2^{\frac{1}{2}} \mathbf{v}_{p,h,2}^n\|_{0,\Omega_2}^2 \\ \lesssim \tau \delta_2 \epsilon_2^{-1} (\alpha_2 \tau + 1)^{-1} \|D_\tau \mathbf{u}_{h,2}^n\|_{0,\Omega_2}^2 + \delta_2 \epsilon_2 \|\mu_2^{-\frac{1}{2}} p_{h,2}^n\|_{0,\Omega_2}^2 .$$

Third term. Thanks to inverse inequalities, it is easily found that $\mathcal{J}_h(q_h, q_h) = \|\mu^{-\frac{1}{2}} [\![q_h]\!]\|_{-\frac{1}{2},h,\mathcal{F}_h}^2 \lesssim \|\mu^{-\frac{1}{2}} q_h\|_{0,\Omega}^2$ for any $q_h \in Q_h$. This implies $\|\mu^{-\frac{1}{2}} [\![(\mu \nabla \cdot \mathbf{u}_h^n)]\!]\|_{-\frac{1}{2},h,\mathcal{F}_h}^2 \lesssim \|\mu^{\frac{1}{2}} \nabla \cdot \mathbf{u}_h^n\|_{0,\Omega}^2$. Similarly, we have

$$\int_\Gamma \{\mu \nabla \cdot \mathbf{u}_h^n\}_w [\![\mathbf{u}_h^n \cdot \mathbf{n}]\!] \lesssim \|\mu^{\frac{1}{2}} \nabla \cdot \mathbf{u}_h^n\|_{0,\Omega} \|\{\mu\}_w^{\frac{1}{2}} [\![\mathbf{u}_h^n \cdot \mathbf{n}]\!]\|_{+\frac{1}{2},h,\Gamma}.$$

Hence, using again the Young's inequality for any $\epsilon_3 > 0$, we have

$$\mathcal{C}_h((\mathbf{u}_h^n, p_h^n), (0, \delta_3 \mu \nabla \cdot \mathbf{u}_h^n)) \ge \delta_3 \big(1 - C_3(\gamma_p + 2)\epsilon_3\big) \|\mu^{\frac{1}{2}} \nabla \cdot \mathbf{u}_h^n\|_{0,\Omega}^2 \\ - C_3 \delta_3 \epsilon_3^{-1} \Big[\gamma_p \|\mu^{-\frac{1}{2}} [\![p_h^n]\!]\|_{-\frac{1}{2},h,\mathcal{F}_h}^2 + \|\mu^{\frac{1}{2}} \mathbf{u}_h^n \cdot \mathbf{n}\|_{+\frac{1}{2},h,\Gamma^D}^2 + \|\{\mu\}_w^{\frac{1}{2}} [\![\mathbf{u}_h^n \cdot \mathbf{n}]\!]\|_{+\frac{1}{2},h,\Gamma}^2 \Big],$$

and no additional terms concerning $D_\tau \mathbf{u}_h^n$ are introduced here.

Combining the three main steps, we find

$$\begin{aligned} D_\tau &\|\mathbf{u}_{h,2}^n\|_{0,\Omega_2}^2 + \tau \big[\tfrac{1}{2} - \delta_2 \epsilon_2^{-1} (\alpha_2 \tau + 1)^{-1}\big] \|D_\tau \mathbf{u}_{h,2}^n\|_{0,\Omega_2}^2 \\ &+ \big[C_{pos} - C_3 \delta_3 \epsilon_3^{-1}\big] \Big(\|\{\mu\}_w^{\frac{1}{2}} [\![\mathbf{u}_h^n]\!] \cdot \mathbf{n}\|_{+\frac{1}{2},h,\Gamma}^2 + \sum_{i=1,2} \|\mu_i^{\frac{1}{2}} \mathbf{u}_{h,i}^n \cdot \mathbf{n}\|_{+\frac{1}{2},h,\Gamma_i^D}^2 \Big) \\ &+ \delta_2 \big[1 - C_2 \epsilon_2\big] \|\mu^{-\frac{1}{2}} p_h^n\|_{0,\Omega}^2 + \big[\gamma_p \big(1 - C_3 \delta_3 \epsilon_3^{-1}\big) - \delta_2 C_2\big] \sum_{i=1,2} \|\mu_i^{-\frac{1}{2}} [\![p_h^n]\!]\|_{-\frac{1}{2},h,\mathcal{F}_{h,i}}^2 \\ &+ \big[C_{pos} - C_2 \delta_2 \epsilon_2^{-1}\big] |||\mathbf{u}_h^n|||^2 + \big[\delta_3 (1 - C_3(\gamma_p + 2)\epsilon_3)\big] \|\mu^{\frac{1}{2}} \nabla \cdot \mathbf{u}_h^n\|_{0,\Omega}^2 \\ &\le |||\mathcal{G}^n|||\, |||(\mathbf{v}_h^n, q_h^n)|||. \end{aligned} \quad (12)$$

Now, let us check that, for a suitable choice of the parameters γ_p, ϵ_i, δ_i $(i = 2,3)$, all terms between square brackets in (12) are positive and upper/lower bounded by constants independent of α, h and τ for any $0 < \tau, h \lesssim 1$. To this end, it suffices to choose for instance $\gamma_p \gtrsim 1$ and

$$\epsilon_2 = \frac{1}{2C_2}, \quad \delta_2 = \frac{1}{C_2} \min\left\{ \frac{1}{8}(\alpha_2\tau + 1), \frac{C_{pos}}{4C_2}, \frac{\gamma_p}{4C_2} \right\}$$
$$\epsilon_3 = \frac{1}{2(\gamma_p + 2)C_3}, \quad \delta_3 = \epsilon_3 \min\left\{ \frac{1}{2C_3}, \frac{C_{pos}}{C_3} \right\}$$

Notice that δ_2 admits upper and lower bound independent of τ. Hence,

$$\begin{aligned} D_\tau\|\mathbf{u}_{h,2}^n\|_{0,\Omega_2}^2 + \tau D_\tau\|\mathbf{u}_{h,2}^n\|_{0,\Omega_2}^2 \\ + \Big[|||\mathbf{u}_h^n|||^2 + \|\mu^{\frac{1}{2}}\mathbf{u}_h^n \cdot \mathbf{n}\|_{+\frac{1}{2},h,\Gamma^D}^2 + \|\{\mu\}_w^{\frac{1}{2}}[\![\mathbf{u}_h^n]\!] \cdot \mathbf{n}\|_{+\frac{1}{2},h,\Gamma}^2 + \|\mu^{\frac{1}{2}}\nabla\cdot\mathbf{u}_h^n\|_{0,\Omega}^2 \\ + \|\mu^{-\frac{1}{2}}p_h^n\|_{0,\Omega}^2 + \|\mu^{-\frac{1}{2}}[\![p_h^n]\!]\|_{-\frac{1}{2},h,\mathcal{F}_h}^2 \Big] \lesssim |||\mathcal{G}^n|||\,|||(\mathbf{v}_h^n, q_h^n)|||. \end{aligned} \quad (13)$$

Moreover, we have

$$|||(\mathbf{v}_h^n, q_h^n)||| \le |||(\mathbf{u}_h^n, p_h^n)||| + \delta_2|||(\mathbf{v}_{p,h}^n, 0)||| + \delta_3|||(0, \mu\nabla\cdot\mathbf{u}_h^n)|||.$$

Using the stabilized inf-sup condition, we have

$$|||(\mathbf{v}_{p,h}^n, 0)||| \lesssim \|\mu^{\frac{1}{2}}\mathbf{v}_{p,h}^n\|_{1,\Omega} \lesssim \|\mu^{-\frac{1}{2}}p_h^n\|_{0,\Omega} \lesssim |||(\mathbf{u}_h^n, p_h^n)|||.$$

It has already been observed that $\|\mu^{-\frac{1}{2}}[\![(\mu\nabla\cdot\mathbf{u}_h^n)]\!]\|_{-\frac{1}{2},h,\mathcal{F}_h} \lesssim \|\mu^{\frac{1}{2}}\nabla\cdot\mathbf{u}_h^n\|_{0,\Omega}$; hence, $|||(0, \mu\nabla\cdot\mathbf{u}_h^n)||| \lesssim |||(\mathbf{u}_h^n, p_h^n)|||$. Since $\delta_i \lesssim 1$, we conclude

$$|||(\mathbf{v}_h^n, q_h^n)||| \lesssim |||(\mathbf{u}_h^n, p_h^n)|||.$$

From this estimate and (13), using Young's inequality we have

$$D_\tau\|\mathbf{u}_{h,2}^n\|_{0,\Omega_2}^2 + \tau\|D_\tau\mathbf{u}_{h,2}^n\|_{0,\Omega_2}^2 + (1-\epsilon)|||\mathbf{u}_h^n, p_h^n|||^2 \lesssim \epsilon^{-1}|||\mathcal{G}^n|||^2 \quad (14)$$

and the result follows summing over the time advancing index for $\epsilon > 0$ small enough. □

4.3 Stability and conditioning of the fully discrete scheme

In this section we focus on problem (9) that has to be solved at each time step. Our starting point is the following equivalence result,

$$1 \lesssim \sup_{0\neq(\mathbf{v}_h,q_h)\in\mathbf{W}_h} \frac{\mathcal{C}_h^\tau((\mathbf{u}_h,p_h),(\mathbf{v}_h,q_h))}{|||\mathbf{u}_h,p_h|||_\tau\,|||\mathbf{v}_h,q_h|||_\tau} \lesssim 1 \quad \forall(\mathbf{u}_h,p_h)\in\mathbf{V}_h\times Q_h. \quad (15)$$

Notice that the upper bound is direct consequence of the boundedness property of Lemma 4.1. The lower bound is a consequence of the stabilized inf-sup condition. More precisely, it follows from eq. (12) of Theorem 4.1, see also [9].

Consider the linear system corresponding to (9). With little abuse of notation, in this section $\mathbf{u}_h \in \mathbf{V}_h$ and $p_h \in Q_h$ will also denote the vectors $\mathbf{u}_h \in \mathbb{R}^{\dim(\mathbf{V}_h)}$ and $p_h \in \mathbb{R}^{\dim(Q_h)}$ associated to the respective finite element bases of the spaces $\mathbf{V}_h$, Q_h. Hence, the matrix form of (9) reads

$$C\begin{bmatrix}\mathbf{u}_h\\ p_h\end{bmatrix} = \begin{bmatrix}\frac{1}{\tau}M + A & B^T\\ -B & J\end{bmatrix}\begin{bmatrix}\mathbf{u}_h\\ p_h\end{bmatrix} = \begin{bmatrix}\mathbf{f}_h\\ g_h\end{bmatrix}, \quad (16)$$

where blocks M, A, B, J and vectors $\mathbf{f}_h$, g_h are defined by the following representation formulas,

$$(\mathbf{u}_h, \mathbf{v}_h)_{0,\Omega_2} = (\mathbf{v}_h, M\mathbf{u}_h)_2, \quad \mathcal{A}_h(\mathbf{u}_h, \mathbf{v}_h) = (\mathbf{v}_h, A\mathbf{u}_h)_2, \quad \mathcal{B}_h(q_h, \mathbf{u}_h) = (q_h, B\mathbf{u}_h)_2,$$

$$\mathcal{J}_h(p_h, q_h) = (q_h, Jp_h)_2, \quad \mathcal{G}(\mathbf{v}_h, q_h) + \frac{1}{\tau}(\mathbf{u}_h^{n-1}, \mathbf{v}_h)_{0,\Omega_2} = (\mathbf{v}_h, \mathbf{f}_h)_2 + (q_h, g_h)_2,$$

where $(\cdot,\cdot)_2$ is the generic Euclidean scalar product in $\mathbb{R}^n$, $n \in \mathbb{N}$. Note that M is a block diagonal mass matrix and the block associated with Ω_1 is zero. Let us equip $\mathbb{R}^{\dim(\mathbf{V}_h)} \times \mathbb{R}^{\dim(Q_h)}$ with the norm defined by

$$|||\mathbf{v}_h, q_h|||_\tau^2 = (\mathbf{v}_h, H_V \mathbf{v}_h)_2 + (p_h, H_Q p_h)_2,$$

being H_V and H_Q the symmetric, positive matrices inducing the natural norms on $\mathbf{V}_h$ and Q_h, i.e.

$$\begin{aligned}
(\mathbf{v}_h, H_V \mathbf{v}_h)_2 &= |||\mathbf{v}_h|||^2 + \|\{\mu\}_w^{\frac{1}{2}} [\![\mathbf{v}_h]\!] \cdot \mathbf{n}\|_{+\frac{1}{2},h,\Gamma}^2 \\
&\quad + \sum_{i=1,2} \left[\|\mu_i^{\frac{1}{2}} \nabla \cdot \mathbf{v}_{h,i}\|_{0,\Omega_i}^2 + \|\mu_i^{\frac{1}{2}} \mathbf{v}_{h,i} \cdot \mathbf{n}\|_{+\frac{1}{2},h,\Gamma_i^D}^2 \right], \\
(p_h, H_Q p_h)_2 &= \sum_{i=1,2} \left[\|\mu_i^{-\frac{1}{2}} q_{h,i}\|_{0,\Omega_i}^2 + \|\mu_i^{-\frac{1}{2}} [\![q_h]\!]\|_{-\frac{1}{2},h,\mathcal{F}_{h,i}}^2 \right].
\end{aligned}$$

Note that, owing to standard inverse inequalities, H_Q is spectrally equivalent to the mass matrix $\tilde{H}_Q$ defined by $(p_h, \tilde{H}_Q p_h)_2 = \sum_{i=1,2} \|\mu_i^{-\frac{1}{2}} q_{h,i}\|_{0,\Omega_i}^2$. Consider the following block-diagonal, symmetric and positive definite matrix,

$$P = \begin{bmatrix} H_V & 0 \\ 0 & H_Q \end{bmatrix}, \quad \text{or} \quad P = \begin{bmatrix} H_V & 0 \\ 0 & \tilde{H}_Q \end{bmatrix}. \tag{17}$$

From eq. (15), we have that for all $\mathbf{u}_h \in \mathbf{V}_h$, $p_h \in Q_h$,

$$\|(\mathbf{u}_h, p_h)\|_2 \lesssim \sup_{\mathbf{v}_h, q_h} \frac{((\mathbf{u}_h, p_h), P^{-\frac{1}{2}} C P^{-\frac{1}{2}} (\mathbf{v}_h, q_h))_2}{\|(\mathbf{v}_h, q_h)\|_2} \lesssim \|(\mathbf{u}_h, p_h)\|_2.$$

Thanks to these bounds, we have that the singular values of the matrix $P^{-\frac{1}{2}} C P^{-\frac{1}{2}}$ are lower and upper bounded by positive constants $\underline{\sigma}$, $\overline{\sigma}$ independent of h, τ, α (see also [3], section II.3.1, and [9], section 3 and theorem 3.8). It follows that $\underline{\sigma} \leq |\lambda_i(P^{-1}C)| \leq \overline{\sigma}$, being $\lambda_i(P^{-1}C)$ the eigenvalues of the preconditioned matrix $P^{-1}C$. As a consequence, P-preconditioned Krylov methods can be successfully employed to solve problem (9) at each time step: for a fixed tolerance, we expect the number of iterations to be almost independent of the discretization and physical parameters. This is confirmed by the numerical experiments of section 6.1 (see Tables 1 and 2).

The preconditioner P has a block-diagonal structure, each block being a symmetric positive definite matrix (SPD). The pressure block is (equivalent to) a pressure mass matrix: it can be lumped and easily inverted. The velocity block is more challenging. In spite of the good SPD property, it features a div-div term $\sum_{i=1,2} (\mu_i \nabla \cdot \mathbf{u}_{h,i}, \nabla \cdot \mathbf{v}_{h,i})_{0,\Omega_i}$. Due to its large kernel, this term makes system (16) to be severely ill conditioned, when the coefficients μ_i become large. As a result, suitable sub-preconditioners have to be used to efficiently solve systems associated to matrix H_V. The failure of standard Incomplete LU (ILU) or Incomplete Cholesky (IC) factorization in such case is well known. A detailed analysis and an effective preconditioning strategy has been proposed by Arnold in [1], owing to a suitable multigrid V-cycle.

Similar problems are encountered when considering Schur complement preconditioners, i.e. choosing

$$P = \begin{bmatrix} \frac{1}{\tau} M + A & 0 \\ B & -\hat{S} \end{bmatrix}$$

where $\hat{S}$ is a preconditioner for $S = B\left(\frac{1}{\tau}M + A\right)^{-1}B^T + J$. For a stationary pure Stokes' problem, S is spectrally equivalent to a pressure mass matrix also in our stabilized case [9]. However, if a Darcy's permeability term or a time discretization term is considered, this equivalence is lost. As pointed out in [12] for the time dependent Stokes equation, a technique first proposed by Cahouet-Chabard [7] can be effectively employed to devise optimal preconditioners also in the limit of τ small, when the algebraic problem to be solved is substantially equivalent to a Darcy's problem. It consists in preconditioning the Schur complement S using a weighted combination of the pressure mass matrix and a pressure discrete Laplacian. In our case, discontinuous pressure is nonconformal to H^1, so that a "cheaper" discrete Laplace operator is not immediately available. For a class of stable finite element pairs, this problem has been investigated in [15] where spectral equivalence with an interior penalty discrete Laplace operator has been shown. Unfortunately this result does not apply to our stabilized pair. As observed in [9], using the modified complement $B\tilde{H}_Q^{-1}B^T + J$ as a discrete Laplace operator on the pressure space is optimal, but stiff. In fact, it was shown that in order to solve the related linear system by IC-preconditioned CG method within a fixed number of iterations, the threshold and fill-in parameters of the IC factorization of $B\tilde{H}_Q^{-1}B^T + J$ have to accommodate for an increasing percentage of non-zero entries as $h \to 0$, resulting in a considerable augmentation of allocated memory as the mesh is refined.

In the 3D numerical simulations presented in the last section of this paper, the preconditioning issue has been one of the most important at the linear algebra level. As a trade-off between the solution of the full saddle-point problem with direct methods and the use of complex multigrid preconditioners, we resorted to a sparse multifrontal factorization of the block H_V to be precomputed off-line, and GMres iterations using the block-diagonal preconditioner P of eq. (17). The price to be payed for this optimal preconditioner is an important increase in memory needs compared to those of standard incomplete factorizations.

5 Error analysis

5.1 Convergence analysis for the fully-implicit scheme

The error analysis of parabolic problems can be split into the analysis of the time discretization error and the analysis related to spatial approximation. The former task, substantially relies on the stability estimate that we have presented in Theorem 4.1. The latter analysis is based on the standard approximation properties of the finite element space. However, we remind that $|||\mathbf{v}_h, q_h|||$ is a mesh dependent norm affected by the values of h and τ. This represents a difficulty for the convergence analysis that will be carefully addressed in what follows. To this purpose we introduce the following (scheme dependent) Ritz projection operator (for any $\epsilon > 0$):

$$S_h := P_h \times R_h : \left(\mathbf{V} \cap \mathbf{H}^{\frac{3}{2}+\epsilon}(\Omega_2)\right) \times \left(Q \cap H^{\frac{1}{2}+\epsilon}(\Omega_2)\right) \to (\mathbf{V}_h \cap \mathbf{V}) \times Q_h$$

such that for any $(\mathbf{u}, p)$ the projection $S_h(\mathbf{u}, p) := \big(P_h(\mathbf{u}, p), R_h(\mathbf{u}, p)\big)$ is defined as the unique solution of

$$\mathcal{C}_h\big(S_h(\mathbf{u}, p), (\mathbf{v}_h, q_h)\big) = \mathcal{C}_h\big((\mathbf{u}, p), (\mathbf{v}_h, q_h)\big)\ \forall (\mathbf{v}_h, q_h) \in (\mathbf{V}_h \cap \mathbf{V}) \times Q_h. \quad (18)$$

For the well posedness of problem (18) we rely on the stability property in the norm $|||\mathbf{v}_h, q_h|||$, for which we refer to Lemma 2.3 of [9] or Theorem 4.8 [10]. Then, we introduce the following auxiliary result.

Lemma 5.1 (Approximation) *Provided that* $(\mathbf{u}_i, p_i) \in L^\infty\big((0,T];(\mathbf{H}^2(\Omega_i)\cap\mathbf{V}_i)\times H^1(\Omega_i)\big)$ *for* $i = 1,2$ *and for the particular weights*

$$w_1 := \frac{\mu_2}{\mu_1+\mu_2},\ w_2 := 1 - w_1 = \frac{\mu_1}{\mu_1+\mu_2}$$

there exists constant $C(\alpha) > 0$ *that directly depends on* α *solely such that,*

$$|||(I-P_h)(\mathbf{u},p),(I-R_h)(\mathbf{u},p)|||^2_{S_h} \le C(\alpha)h^2 \sum_{i=1,2}\Big(|\mathbf{u}_i|^2_{2,\Omega_i} + |p_i|^2_{1,\Omega_i}\Big), \tag{19}$$

where $|||(\mathbf{v}_h, q_h)|||_{S_h}$ *denotes the following norm*

$$|||(\mathbf{v}_h,q_h)|||^2_{S_h} := |||\mathbf{v}_h|||^2 + \|\{\mu\}_w^{\frac12}[\![\mathbf{v}_h]\!]\cdot\mathbf{n}\|^2_{+\frac12,h,\Gamma}$$
$$+\sum_{i=1,2}\Big[\|\overline{\mu}_i^{\frac12}\nabla\cdot\mathbf{v}_{h,i}\|^2_{0,\Omega_i} + \|\overline{\mu}_i^{\frac12}\mathbf{v}_{h,i}\cdot\mathbf{n}\|^2_{+\frac12,h,\Gamma_i^D} + \|\mu_i^{-\frac12}q_{h,i}\|^2_{0,\Omega_i} + \|\mu_i^{-\frac12}[\![q_h]\!]\|^2_{-\frac12,h,\mathcal{F}_{h,i}}\Big],$$

with $\overline{\mu}_1 = 1$ *and* $\overline{\mu}_2 = \alpha_2$*, which trivially satisfies* $|||(\mathbf{v}_h,q_h)|||_{S_h} \le |||(\mathbf{v}_h,q_h)|||$ *for any* $(\mathbf{v}_h,q_h) \in \mathbf{W}_h$*. In addition, if* $\partial_t\mathbf{u}_2 \in L^2\big((0,T];\mathbf{H}^2(\Omega_2)\big)$ *and* $\partial_t p_2 \in L^2\big((0,T];H^1(\Omega_2)\big)$ *we have,*

$$\int_0^T \|\partial_t(I-P_{h2})(\mathbf{u},p)\|^2_{0,\Omega_2} \le h^2\int_0^T\Big(|\partial_t\mathbf{u}_2|^2_{2,\Omega_2} + |\partial_t p_2|^2_{1,\Omega_2}\Big). \tag{20}$$

Proof. We obtain the desired result following the lines of [10], Theorem 4.10, under the required regularity assumptions. We notice that the projection error $|||(I-P_h)(\mathbf{u},p),(I-R_h)(\mathbf{u},p)|||_{S_h}$ directly depends on $\alpha_i, \mu_i^{-1}, \{\mu\}_w$ solely. Provided that the averaging weights w_i are selected as indicated, these quantities are uniformly bounded with respect to τ with constants that only depend on the parameter α. Finally, the proof of (20) follows from (19) combined with the commutativity between the time derivative ∂_t and the operator $(I - P_{hi})$. □

Remark 5.1 We point out that the $|||\cdot|||_{S_h}$ norm is slightly weaker than its $|||\cdot|||$ counterpart, but the approximation estimate (19) with $C(\alpha)$ uniformly bounded as $\tau \to 0$ holds in the S_h norm only, because $|||(\mathbf{v}_h,q_h)|||^2 = |||(\mathbf{v}_h,q_h)|||^2_{S_h} + \|\tau^{-\frac12}\nabla\cdot\mathbf{v}_{h,2}\|^2_{0,\Omega_2} + \|\tau^{-\frac12}\mathbf{v}_{h,2}\cdot\mathbf{n}\|^2_{+\frac12,h,\Gamma_2^D}$.

Before proceeding, we introduce the following notation. Let $\langle\cdot,\cdot\rangle$ be the duality pairing between $H^1(\Omega)$ and its dual space, denoted with $H^*(\Omega)$. Then, for any $\phi_2 \in H^*(\Omega_2)$ we set

$$\|\phi_2\|_{-1,h,\Omega_2} := \sup_{\mathbf{v}_{h,2}\in\mathbf{V}_{h,2}}\{\langle\phi_2,\mathbf{v}_{h,2}\rangle:\ \|\alpha_2^{\frac12}\mathbf{v}_{h,2}\|_{1,\Omega_2}\le 1\}$$

which is a norm on $\mathbf{V}_{h,2}$ such that $\|\phi_2\|_{-1,h,\Omega_2} \le \alpha_2^{-\frac12}\|\phi_2\|_{0,\Omega_2}$.

Theorem 5.1 (Convergence) *Let* $(\mathbf{u},p)$ *be the weak solution of problem* (5) *with the additional regularity assumption* (6)*. Under the assumptions of Lemma 4.1 for all* $n = 0,1,\ldots,N_\tau = \frac{T}{\tau}$ *we have*

$$\|\mathbf{u}_2(t_n) - \mathbf{u}^n_{h,2}\|^2_{0,\Omega_2} + \tau\sum_{k=1}^n |||\mathbf{u}(t_k)-\mathbf{u}^k_h, p(t_k)-p^k_h|||^2_{S_h}$$
$$\lesssim \tau^2\int_{t_0}^{t_n}\|\partial_{tt}\mathbf{u}_2(s)\|^2_{-1,h,\Omega_2}\,ds + \mathcal{E}^n_h(\mathbf{u},p), \tag{21}$$

where, given $\mathbf{u}_{2,0}$ *and* $p_{2,0} = 0$, $\mathcal{E}_h^n(\mathbf{u}, p)$ *accounts for the accumulation of the spatial error from* t_0 *until* t_n *and it is equivalent to*

$$\mathcal{E}_h^n(\mathbf{u}, p) := \|P_{h2}(\mathbf{u}_{2,0}, 0) - \mathbf{u}_{h,2}^0\|_{0,\Omega_2}^2 + \alpha^{-2} \int_{t_0}^{t_n} \|\partial_t (I - P_{h2})(\mathbf{u}(s), p(s))\|_{0,\Omega_2}^2 \, ds$$
$$+ \|(I - P_{h2})(\mathbf{u}(t_n), p(t_n))\|_{0,\Omega_2}^2 + \tau \sum_{k=1}^{n} |||(I - P_h)(\mathbf{u}, p), (I - R_h)(\mathbf{u}, p)|||_{S_h}^2.$$

Furthermore, under the assumptions of Lemma 5.1 and provided that $\mathbf{u}_{2,0} \in \mathbf{H}^2(\Omega_2)$ *we obtain,*

$$\begin{aligned} \mathcal{E}_h^n(\mathbf{u}, p) \lesssim \; & h^2 \Big[|\mathbf{u}_{2,0}|_{1,\Omega_2}^2 + C(\alpha) |\mathbf{u}_{2,0}|_{2,\Omega_2}^2 \Big] \\ & + h^2 \Big[C(\alpha) \sup_{t \in (t_0, t^n]} \sum_{i=1,2} \big(|\mathbf{u}_i(t)|_{2,\Omega_i}^2 + |p_i(t)|_{1,\Omega_i}^2 \big) \\ & + \int_{t_0}^{t_n} \Big(|\partial_t \mathbf{u}_2(s)|_{2,\Omega_2}^2 + |\partial_t p_2(s)|_{1,\Omega_2}^2 \Big) ds \Big]. \end{aligned} \tag{22}$$

Proof. Let us split the error $(\mathbf{w}(t_n), r(t_n)) := (\mathbf{u}(t_n), p(t_n)) - (\mathbf{u}_h^n, p_h^n)$ as follows,

$$\begin{aligned} (\mathbf{w}^n, r^n) &:= ((I - P_h(\mathbf{u}(t_n), p(t_n))), (I - R_h(\mathbf{u}(t_n), p(t_n)))), \\ (\mathbf{w}_h^n, r_h^n) &:= (P_h(\mathbf{u}(t_n), p(t_n)), R_h(\mathbf{u}(t_n), p(t_n))) - (\mathbf{u}_h^n, p_h^n), \end{aligned}$$

Starting from (9) and exploiting $\mathbf{u}_h^k = P_h(\mathbf{u}(t_k), p(t_k)) - \mathbf{w}_h^k$ we have:

$$\begin{aligned} \big(D_\tau \mathbf{w}_{h,2}^n, \mathbf{v}_{h,2}\big)_{\Omega_2} = \; & \big(D_\tau P_{h2}(\mathbf{u}(t_n) p(t_n)), \mathbf{v}_{h,2}\big)_{\Omega_2} \\ & + \mathcal{C}_h((\mathbf{u}_h^n, p_h^n), (\mathbf{v}_h, q_h)) - \mathcal{G}^n(\mathbf{v}_h, q_h). \end{aligned}$$

Then, exploiting the consistency of the finite element scheme, see Lemma 4.1, we obtain

$$\begin{aligned} \big(D_\tau \mathbf{w}_{h,2}^n, \mathbf{v}_{h,2}\big)_{\Omega_2} = \; & \big(D_\tau P_{h2}(\mathbf{u}(t_n), p(t_n)), \mathbf{v}_{h,2}\big)_{\Omega_2} \\ & - \big(\partial_t \mathbf{u}_2(t_n), \mathbf{v}_{h,2}\big)_{\Omega_2} - \mathcal{C}_h((\mathbf{w}(t_n), r(t_n)), (\mathbf{v}_h, q_h)), \end{aligned}$$

and replacing $P_{h2}(\mathbf{u}(t_n), p(t_n)) = \mathbf{u}(t_n) - \mathbf{w}^n$ we end up with

$$\big(D_\tau \mathbf{w}_{h,2}^n, \mathbf{v}_{h,2}\big)_{\Omega_2} + \mathcal{C}_h((\mathbf{w}_h^n, r_h^n), (\mathbf{v}_h, q_h)) = \mathcal{R}^n(\mathbf{v}_h, q_h) \tag{23}$$

where, thanks to (18), we have

$$\begin{aligned} \mathcal{R}^n(\mathbf{v}_h, q_h) &:= \langle \boldsymbol{z}_h^n, \mathbf{v}_h \rangle - \mathcal{C}_h((\mathbf{w}^n, r^n), (\mathbf{v}_h, q_h)) = \langle \boldsymbol{z}_h^n, \mathbf{v}_h \rangle, \\ \boldsymbol{z}_{h,2}^n &:= (D_\tau - \partial_t)\mathbf{u}_2(t_n) - D_\tau \mathbf{w}_2^n, \quad \boldsymbol{z}_{h,1}^n := 0. \end{aligned}$$

We rewrite the residual term as follows,

$$\boldsymbol{z}_{h,2}^n = \frac{1}{\tau} \int_{t_{n-1}}^{t_n} (t_n - s) \partial_{tt} \mathbf{u}_2(s) ds - D_\tau \mathbf{w}_2^n \tag{24}$$

Moreover, the discrete time derivative residual can be rearranged as follows

$$\begin{aligned} D_\tau \mathbf{w}_2^n &= \tau^{-1} (I - P_{h2})(\mathbf{u}(t_n) - \mathbf{u}(t_{n-1}), p(t_n) - p(t_{n-1})) \\ &= \frac{1}{\tau} \int_{t_{n-1}}^{t_n} \partial_t (I - P_{h2})(\mathbf{u}(s), p(s)) ds. \end{aligned} \tag{25}$$

We observe that (23) has exactly the same structure as equation (9), where $\mathcal{G}^n(\mathbf{v}_h, q_h)$ is replaced by $\mathcal{R}^n(\mathbf{v}_h, q_h)$. Then, to provide a suitable estimate for $|||\mathcal{R}^n|||$ we combine Cauchy-Schwarz and Poincaré-Friedrichs inequalities,

$$\langle \boldsymbol{z}_{h,2}^n, \mathbf{v}_{h,2}\rangle \leq \|\boldsymbol{z}_{h,2}^n\|_{-1,h,\Omega_2}\Big(\|\alpha_2^{\frac{1}{2}}\nabla\mathbf{v}_{h,2}\|_{0,\Omega_2}^2 + \|\alpha_2^{\frac{1}{2}}\mathbf{v}_{h,2}\|_{\frac{1}{2},h,\Gamma_2^D}^2\Big)$$

and according to the definition of the norm $|||\mathcal{R}^n|||$, we get

$$|||\mathcal{R}^n|||^2 \lesssim \|\boldsymbol{z}_{2,h}^n\|_{-1,h,\Omega_2}^2. \tag{26}$$

Using (24), (25) and following the reasoning developed in [16] we obtain,

$$\|\boldsymbol{z}_{2,h}^n\|_{-1,h,\Omega_2}^2 \leq \tau\int_{t_{n-1}}^{t_n}\|\partial_{tt}\mathbf{u}_2(s)\|_{-1,h,\Omega_2}^2\,ds \\ + \tau^{-1}\alpha_2^{-1}\int_{t_{n-1}}^{t_n}\|\partial_t(I-P_{h2})(\mathbf{u}(s),p(s))\|_{0,\Omega_2}^2\,ds. \tag{27}$$

Thus, proceeding as in Theorem 4.1, we have

$$\|\mathbf{w}_{h,2}^n\|_{0,\Omega_2}^2 + \tau^2\sum_{k=1}^n\|D_\tau\mathbf{w}_{h,2}^k\|_{0,\Omega_2}^2 + \tau\sum_{k=1}^n|||(\mathbf{w}_h^k, r_h^k)|||^2 \\ \lesssim \|\mathbf{w}_{h,2}^0\|_{0,\Omega_2}^2 + \tau\sum_{k=1}^n|||\mathcal{R}^k|||^2.$$

The proof of (21) is concluded using (26) and (27), combined with the triangle inequality applied as follows,

$$\|\mathbf{w}_2(t_n)\|_{0,\Omega_2}^2 + \tau\sum_{k=1}^n|||(\mathbf{w}(t_k), r(t_k))|||_{S_h}^2 \\ \lesssim \|\mathbf{w}_{h,2}^0\|_{0,\Omega_2}^2 + \|\mathbf{w}_2^n\|_{0,\Omega_2}^2 + \tau\sum_{k=1}^n|||\mathbf{w}^k, r^k|||_{S_h}^2 + \tau\sum_{k=1}^n|||\mathcal{R}^k|||^2.$$

Finally, (22) is easily obtained by applying (19) and (20) into (21) under the additional regularity assumptions for the exact solution and its temporal derivatives. A final detail concerns the analysis of the initial error, i.e. $\|\mathbf{w}_{h,2}^0\|_{0,\Omega_2}$. We notice that,

$$\|\mathbf{w}_{h,2}^0\|_{0,\Omega_2} = \|P_{h2}(\mathbf{u}_{2,0}, 0) - \mathbf{u}_{h,2}^0\|_{0,\Omega_2} \\ \leq \|P_{h2}(\mathbf{u}_{2,0}, 0) - \mathbf{u}_{2,0}\|_{0,\Omega_2} + \|\mathbf{u}_{h,2}^0 - \mathbf{u}_{2,0}\|_{0,\Omega_2}.$$

Then, provided that $\mathbf{u}_{2,0} \in \mathbf{H}^2(\Omega_2)$ we have

$$\|\mathbf{u}_{h,2}^0 - \mathbf{u}_{2,0}\|_{0,\Omega_2}^2 = \|(I-\pi_h)\mathbf{u}_{2,0}\|_{0,\Omega_2}^2 \lesssim h^2|\mathbf{u}_{2,0}|_{1,\Omega_2}^2, \\ \|P_{h2}(\mathbf{u}_{2,0}, 0) - \mathbf{u}_{2,0}\|_{0,\Omega_2}^2 \leq C(\alpha)h^2|\mathbf{u}_{2,0}|_{2,\Omega_2}^2,$$

which completes the proof. □

6 Numerical results and applications

The aim of this section is twofold. First, we address numerical tests on a model problem in order to verify the sharpness of the theoretical estimates concerning the stability, the accuracy and the conditioning of the proposed numerical scheme.

Second, we consider a realistic problem arising from hemodynamics coupled with fluid filtration into biological tissues. This will show that the present scheme is capable to capture the characteristics of this delicate problem and it allows for reasonably efficient solvers.

	$\alpha = 10^0$			$\alpha = 10^{-2}$			$\alpha = 10^{-4}$		
k	e_2	E	N_{It}	e_2	E	N_{It}	e_2	E	N_{It}
1	0.15568	0.01797	302	0.06476	0.01552	337	0.06339	0.01512	425
2	0.07497	0.00935	280	0.03271	0.00801	321	0.03211	0.00772	390
4	0.03667	0.00479	252	0.01642	0.00406	294	0.01613	0.00391	401

Table 1: Errors defined in (29) are reported for different values of α, and different discretization parameters k, such that $h = h_0/k$, $\tau = \tau_0/k$. We also show the average preconditioned GMRes iteration count per time step N_{It} (GMRes tolerance was 10^{-12}).

6.1 Numerical validation of the error estimates on a test case.

To start with, we propose an analytical solution of problem (2), (3), (4) under fairly simplified assumptions on the data and on the geometrical setting. Specifically, define the Darcy domain $\Omega_1 = [-1, 0] \times [0, 1]$ and the Stokes domain $\Omega_2 = [0, 1] \times [0, 1]$, and consider the following functions,

$$\begin{aligned} \mathbf{u}_1 &= \begin{bmatrix} y(1-y) + x^2 + k\cos t \\ (1-2y)x \end{bmatrix}, \quad & p_1 &= -y(1-y)x - kx\cos t - \frac{1}{3}x^3 \\ \mathbf{u}_2 &= \begin{bmatrix} y(1-y) + k\cos t \\ 0 \end{bmatrix}, \quad & p_2 &= (-2\alpha^2 + k\sin t)x, \end{aligned} \tag{28}$$

where k is a constant parameter. Note that for all values of k we have

$$\mathbf{u}_1 + \nabla p_1 = \mathbf{0}, \quad \nabla \cdot \mathbf{u}_1 = 0, \quad \partial_t \mathbf{u}_2 - \alpha^2 \Delta \mathbf{u}_2 + \nabla p_2 = \mathbf{0}, \quad \nabla \cdot \mathbf{u}_2 = 0.$$

Moreover, an easy calculation shows that on $\Gamma = \{0\} \times [0, 1]$ we have

$$\begin{aligned} &\mathbf{u}_1 \cdot \mathbf{e}_x = y(1-y) + k\cos t = \mathbf{u}_2 \cdot \mathbf{e}_x, \quad \mathbf{e}_x \times \mathbf{u}_1 = \mathbf{0}, \\ &\mathbf{e}_x^T \sigma_1 \mathbf{e}_x = p_1 = 0 = \mathbf{e}_x^T \sigma_2 \mathbf{e}_x = p_2 - \alpha^2 \partial_x (\mathbf{u}_1 \cdot \mathbf{e}_x), \end{aligned}$$

where $\mathbf{e}_x = [1, 0]^T = \mathbf{n}_1$, so that (28) satisfies problem (2), (3), (4).

In order to verify the validity of Theorem 5.1, we focus on the left-hand side of (21) and we compute

$$e_2 := \|\mathbf{u}_2(t_N) - \mathbf{u}_{h,2}^N\|_{0,\Omega_2}, \tag{29a}$$

$$E := \left[\tau \sum_{k=1}^{N} |||\mathbf{u}(t_k) - \mathbf{u}_h^k, p(t_k) - p_h^k|||_{S_h}^2 \right]^{\frac{1}{2}} \tag{29b}$$

where N is such that hat $T = N\tau$. To this purpose, we apply different values of α and of $h = h_0/k$, $\tau = \tau_0/k$, with $k = 1, 2, 4$.

The obtained results are shown in table 1. The first order convergence rate is confirmed for all considered values of α (ranging from 10^0 to 10^{-4}). Moreover, the number of preconditioned GMRes iterations to solve the monolithic problems is independent of the discretization parameters and of α. Together with table 2, quantifying the spectrum of the preconditioned problem, this confirms that the proposed method and the related preconditioning strategy are robust with respect to the discretization and physical parameters, also in the strongly heterogeneous case of $\alpha \ll 1$.

k	$\alpha = 10^0$	$\alpha = 10^{-2}$	$\alpha = 10^{-4}$
1	(0.178683, 4.997619)	(0.178708, 4.998270)	(0.178708, 4.998451)
2	(0.178021, 4.999600)	(0.178024, 4.999757)	(0.178024, 4.999785)
4	(0.177840, 4.999928)	(0.177840, 4.999967)	(0.177840, 4.999972)

Table 2: The smallest and largest magnitude $(\lambda_{\min}, \lambda_{\max})$ of the generalized eigenvalue problem $C\mathbf{w} = \lambda P\mathbf{w}$, being P the block-diagonal, symmetric and positive defined matrix defined by (17) (with the pressure block given by $\tilde{H}_Q$). The eigenvalues have been computed using Matlab/Arpack (command `eigs`).

6.2 Application to blood flow and intramural plasma filtration

We implemented the time dependent scheme (9) to study a realistic three-dimensional coronary artery containing a *stent*, i.e. a biomedical device inserted to keep the arterial lumen open after an occlusion (*stenosis* has occurred. The geometry of lumen Ω_l and of the wall Ω_w have been obtained by the simulation of the mechanical expansion of a stent similar to the coronary Cordis BX-Velocity (Johnson & Johnson, Interventional System, Warren, NJ, USA), see [19]. The radius of the lumen is about 1.55 mm, the thickness of the wall is 0.5 mm.

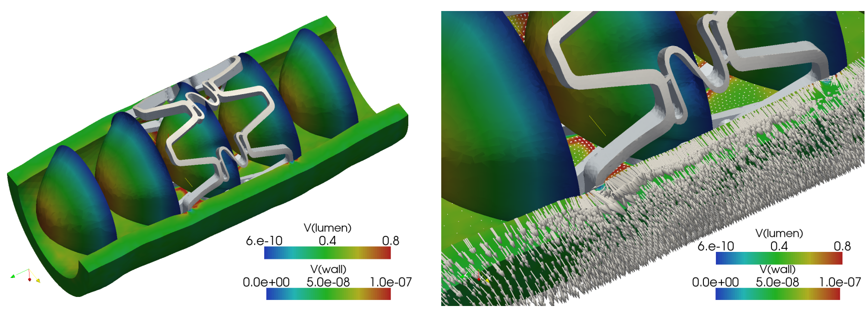

(a) (b)

Figure 1: (a) Problem geometry: we show the magnitude of the wall filtration velocity in the arterial wall, the stent, and luminal velocity profiles at different cross-sections, at a given time step. Note the increased filtration velocity near the DES due to the interaction of transmural pressure gap and the obstacle. (b) Close-up of the device: filtration velocity is represented by vectors.

Assuming that the dynamic viscosity of blood is $\hat{\nu}_2 = 3$ mm^{2}s^{-1} and the inverse permeability of the arterial wall is $\hat{\eta}_1 = 10^{12}$s^{-1}, see [17], taking $\bar{L} = 1$ mm as reference length and $\bar{U} = 250$ mm s^{-1} as reference velocity (corresponding to order of the peak velocity in coronary arteries), we obtain a very small non-dimensional viscosity, $\alpha^2 = 3 \cdot 10^{-12}$. The reference time is also small, $\bar{T} = 10^{-12}$ s.

At the inflow of the lumen we impose a parabolic velocity profile, and consider the representative velocity waveform with mean value 0.5 shown in figure 2(d). The imposed external pressure on the arterial wall was $-2.59 \cdot 10^{-8}$ in our non-dimensional units ($\simeq -50$ mmHg). The hydraulic impedance of circulation downstream the artery has been accounted for by a resistive Robin boundary condition at the outlet, i.e. $\sigma_2(\mathbf{v}_2, p_2)\mathbf{n} = r\mathbf{v}_2$ with $r = -2.28 \cdot 10^{-9}$.

In the physical time domain, we aim to perform 20 time steps per heart beat, which correspond to $\hat{\tau} = 0.05$ s, assuming that the frequency of the heart is 1 Hz. In the non-dimensional framework, the final time of the simulation becomes $T = 10^{12}$

and the non-dimensional time step is $\tau = 5 \cdot 10^{10}$. Using a very large time step is allowed thanks to the absolute stability properties of our scheme.

We have performed a time dependent blood flow simulation, with stabilization parameters given by $\gamma_u = \gamma_p = 10$. Following [9], we have included in our model a nonlinear convective term (Navier-Stokes equation), that we have treated semi-explicitly at each time step. The iterative technique presented in [10, 9] to solve the fully coupled problem by a sequence of local subproblems has also been applied. Moreover, the GMRes method preconditioned by block matrix P of eq. (17) has been used at each time step; the related iteration count was always below 500. As discussed in section 4.3, using an efficient solver for the H_V block is mandatory. We have resorted to a sparse direct method (we used the `MUMPS` multifrontal solver, `http://graal.ens-lyon.fr/MUMPS/`).

Figure 2 shows some typical features of the blood flow around the implanted device at different times. In particular, we observe that recirculation zones appear in proximity of the stent struts at the first part of the heart beat, as it happens in the steady case, while these flow structures are considerably weakened at the end of the period. We also detect small perturbations on the plasma filtration velocity in the arterial wall in the neighborhood of the device, which acts as an obstacle for the flow.

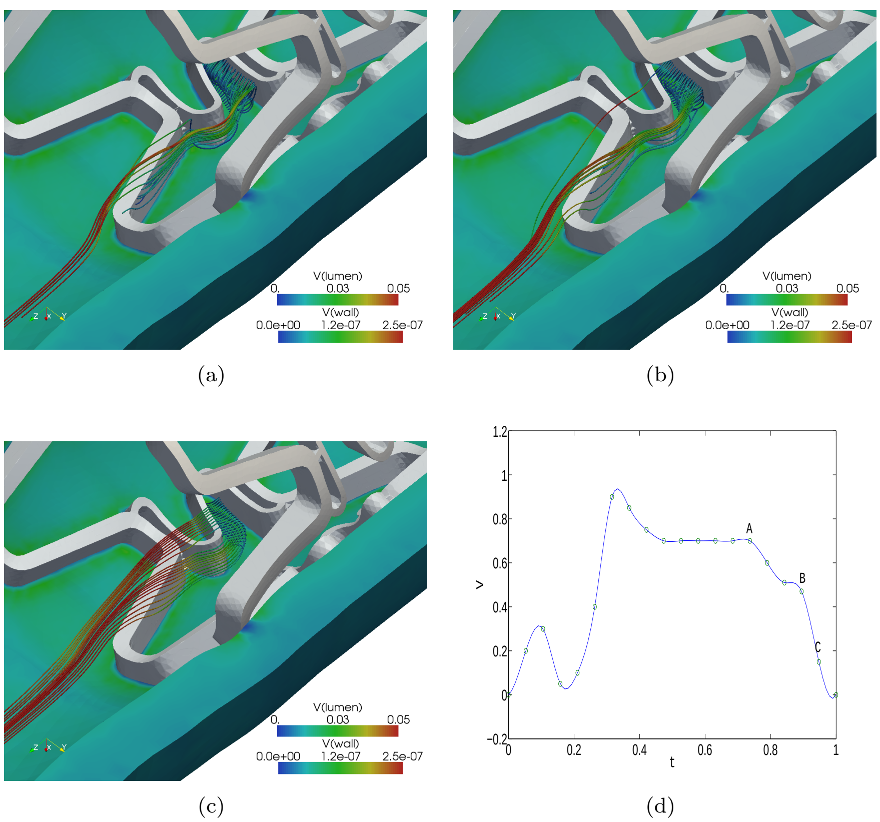

Figure 2: (a,b,c) Blood flow streamlines near the stent at different times (marked in (d)). (d) Inflow velocity waveform over a time period (heart beat).

7 Conclusions

In this work, we proposed a finite element / backward Euler scheme for the approximation of coupled Stokes'-Darcy's transient flow problems. Suitable weights are used to enforce the problem coupling, to define natural norms for the unknowns, and to obtain stability properties that are robust with respect to the physical parameters. Among different choices, we studied a particular formulation in which the weights depend on the time step, in order to achieve unconditional stability and recover effective preconditioning strategies to solve the associated discrete problem. Numerical experiments confirm the predicted features of our scheme, such as convergence rates in suitable weighted norms and conditioning of the discrete problem. The scheme was successfully applied to the computational study of transient blood flow and transmural filtration in a stented artery.

7.1 Acknowledgments

This work has been supported by the Italian Institute of Technology with the project *NanoBiotechnology - Models and methods for biodegradable materials*, and the ERC Advanced Grant N.227058 *MATHCARD - Mathematical Modelling and Simulation of the Cardiovascular System*.

References

[1] Douglas N. Arnold, Richard S. Falk, and R. Winther. Preconditioning in $H(\mathrm{div})$ and applications. *Math. Comp.*, 66(219):957–984, 1997.

[2] Roland Becker, Peter Hansbo, and Rolf Stenberg. A finite element method for domain decomposition with non-matching grids. *M2AN Math. Model. Numer. Anal.*, 37(2):209–225, 2003.

[3] F. Brezzi and M. Fortin. *Mixed and hybrid finite element methods*, volume 15 of *Springer Series in Computational Mathematics*. Springer-Verlag, New York, 1991.

[4] E. Burman and P. Hansbo. A unified stabilized method for Stokes' and Darcy's equations. *J. Comput. Appl. Math.*, 198(1):35–51, 2007.

[5] E. Burman and P. Zunino. A domain decomposition method based on weighted interior penalties for advection-diffusion-reaction problems. *SIAM J. Numer. Anal.*, 44(4):1612–1638, 2006.

[6] Erik Burman and Miguel A. Fernández. Galerkin finite element methods with symmetric pressure stabilization for the transient Stokes equations: stability and convergence analysis. *SIAM J. Numer. Anal.*, 47(1):409–439, 2008/09.

[7] J. Cahouet and J.-P. Chabard. Some fast 3D finite element solvers for the generalized Stokes problem. *Internat. J. Numer. Methods Fluids*, 8(8):869–895, 1988.

[8] Jeffrey M. Connors, Jason S. Howell, and William J. Layton. Partitioned time stepping for a parabolic two domain problem. *SIAM J. Numer. Anal.*, 47(5):3526–3549, 2009.

[9] C. D'Angelo and P. Zunino. Robust numerical approximation of coupled stokes and darcy flows applied to vascular hemodynamics and biochemical transport. Technical Report 35/2009, MOX-Report, 2009. under revision on M2AN.

[10] Carlo D'Angelo and Paolo Zunino. A finite element method based on weighted interior penalties for heterogeneous incompressible flows. *SIAM J. Numer. Anal.*, 47(5):3990–4020, 2009.

[11] John G. Heywood and Rolf Rannacher. Finite element approximation of the nonstationary Navier-Stokes problem. I. Regularity of solutions and second-order error estimates for spatial discretization. *SIAM J. Numer. Anal.*, 19(2):275–311, 1982.

[12] Kent-Andre Mardal and Ragnar Winther. Uniform preconditioners for the time dependent Stokes problem. *Numer. Math.*, 98(2):305–327, 2004.

[13] Karl Perktold, Martin Prosi, and Paolo Zunino. Mathematical models of mass transfer in the vascular walls. In *Cardiovascular mathematics*, volume 1 of *MS&A. Model. Simul. Appl.*, pages 243–278. Springer Italia, Milan, 2009.

[14] Alfio Quarteroni and Alberto Valli. *Numerical approximation of partial differential equations*, volume 23 of *Springer Series in Computational Mathematics*. Springer-Verlag, Berlin, 1994.

[15] Torgeir Rusten, Panayot S. Vassilevski, and Ragnar Winther. Interior penalty preconditioners for mixed finite element approximations of elliptic problems. *Math. Comp.*, 65(214):447–466, 1996.

[16] Jie Shen. On error estimates of projection methods for Navier-Stokes equations: first-order schemes. *SIAM J. Numer. Anal.*, 29(1):57–77, 1992.

[17] S. Tada and J.M. Tarbell. Internal elastic lamina affects the distribution of macromolecules in the arterial wall: a computational study. *Am. J. Physiol. Heart Circ. Physiol.*, 287:H905–H913, 2004.

[18] Vidar Thomée. *Galerkin finite element methods for parabolic problems*, volume 25 of *Springer Series in Computational Mathematics*. Springer-Verlag, Berlin, second edition, 2006.

[19] P. Zunino, C. D'Angelo, L. Petrini, C. Vergara, C. Capelli, and F. Migliavacca. Numerical simulation of drug eluting coronary stents: mechanics, fluid dynamics and drug release. *Comput. Methods Appl. Mech. Engrg.*, 198(45-46):3633–3644, 2009.

MOX Technical Reports, last issues

Dipartimento di Matematica "F. Brioschi",
Politecnico di Milano, Via Bonardi 9 - 20133 Milano (Italy)

22/2010 Carlo D'Angelo, Paolo Zunino:
Numerical approximation with Nitsche's coupling of transient Stokes'/Darcy's flow problems applied to hemodynamics

21/2010 Niccolo' Grieco, Francesca Ieva, Anna Maria paganoni:
Provider Profiling Using Mixed Effects Models on a Case Study concerning STEMI Patients

20/2010 Fabio Nobile, Alfio Quarteroni, Ricardo Ruiz Baier:
Numerical solution of an active strain formulation for the electro-mechanical activity in the heart

19/2010 Loredana Gaudio, Alfio Quarteroni:
hN-adaptive spectral element discretization of optimal control problems for environmental applications

18/2010 Paola F. Antonietti, Nur Aiman Fadel, Marco Verani:
Modelling and numerical simulation of the polymeric extrusion process in textile products

17/2010 Alessandra Guglielmi, Francesca Ieva, Anna Maria Paganoni, Fabrizio Ruggeri:
A Bayesian random-effects model for survival probabilities after acute myocardial infarction

16/2010 Luca Formaggia, Anna Scotti:
Positivity and conservation properties of some integration schemes for mass action kinetics

15/2010 Alfio Quarteroni, Luca Formaggia:
Domain Decomposition (DD) methods

14/2010 Paola F. Antonietti, Lourenco Beirão da Veiga, Marco Verani:
A Mimetic Discretization of Elliptic Obstacle Problems

13/2010 G.M. Porta, Simona Perotto, F. Ballio:
A Space-Time Adaptation Scheme for Unsteady Shallow Water Problems